Journal of Material Sciences & Engineering

Research Article　　　　　　　　　　　　　　　　　　　　　　　　　　　**Open Access**

Laser Induced Shock Wave Studies of Para and Ferro Magnetic Materials

Walid K Hamoudi, Dayah N Raouf and Narges Zamil*

Applied Sciences Department, University of Technology, Baghdad, Iraq

Abstract

In the present work, laser induced shock wave on different materials was studied, the used materials is [Paramagnetic metal (Stainless steel 304) and Ferro magnetic metals (Iron)]; immersed in some media (air and water) to study the media effect on its properties. These materials are irradiated by using different laser intensities. Laser induced shock wave was achieved by employing Nd-YAG laser at wavelength 1064 nm. X-ray diffraction revealed shifting in diffracted angles of Fe toward higher angles due to phase transformation where in air transition from Austenite to Martensite while in water from Martensite to Martensite has smaller grain size because high generated temperature followed by quenched, the diffracted angle of S.S.304 metal shifted toward very little value due to twining effects where high stress and strain are produced.

Keywords: Laser induced shock wave; Hardening; XRD of shocked and un-shocked metal

Introduction

Laser Shock Peening or Laser Shockwave Processing (LSP) is one of three processes of laser-induced shock waves in deformation processing. It is similar to Shot Peening (SP), but laser pulses replace the shots [1]. LSP is a cold work process in which a high-intensity laser pulse hits the selected surface, and then shock waves are generated [2]. LSP applies a force to the selected part of a surface, resulting in a mechanical energy applied to the surface [3]. In solid alloys; like aluminum, the surface depresses little, but depression becomes deep when increasing the treating laser intensity [4]. LSP is an effective life extension technology of fatigue life (very important property of aircraft machinery) because of the deeper residual stresses and a surface finish improves relative to conventional SP. This enhances fatigue life by modifying microstructure and/or compressive residual stresses in the surfaces/sub-surfaces [1-4].

Experimental Section

This section describes all of the tools and equipment used in the generation of the shock wave as well as the techniques used to study and explain the impact of the shock wave on the properties of the materials under study. The Laser system consisted from nanosecond Q-S Nd: YAG laser system; made by (DELIXI) company was utilized in this work. This laser system is working at 1064 nm wavelength and giving laser energy ranging between (1-500) mJ. This laser system provides short 7 ns pulses at 10 repetition frequency. The laser is facilitated with closed system cooling and has the ability of second harmonic generation, but this was not used in the present work. To achieve a high level of laser intensities, this laser is equipped with some focusing lenses made of high optical quality and high damage threshold ED2 glass. Its front panel accommodates a digital readout for the selected laser energy and controlling knobs for pulse repletion frequency and the number of pulses required per one firing touch. A straight forward set-up was adopted in this study. The set-up consists of Nd: YAG laser source, high quality, 10 cm focal length lens, and samples; cut with relevant dimensions to fit the experiment requirement. The laser source was vertically mounted in a holder above the sample, aligned and focused by 10 cm lens to achieve a circular spot with a suitable intensity. Figure 1 show the setup used in our experiments.

Sample Preparation

In this work, the laser-induced shock wave effect on different materials in different media (air, water, and ethanol) was tested. The metals were classified into; Paramagnetic metal (S.S. 304), Ferromagnetic metals (Fe). Some of the used materials were thin plates (Iron, Stainless steel). Each material was prepared in specific dimension to fit the measurement's type required. For structures and morphology measurement, the samples were cut in (1×2) cm². This was followed by polishing them by using graded Amery papers in the range (220-2000), then immersed in diluted HF acid in water (1:50) ml to remove dirt and the native oxide layer. The preparation process was finalized by putting them in an ultrasonic ethanol bath for about 30 min. The used materials can be summarized in the present work as follow: Fe and stainless steel have thick native oxide layer. Getting rid of oxide layer necessitated the use of a combination of Amery paper with benzene, in addition to an ultrasonic bath for 30 min. To complete the cleaning process, these samples also required etching for about 10 seconds in diluted HF: Water (1:10) percent followed by thorough rinsing in water and then in ethanol ultrasonic bath with ethanol.
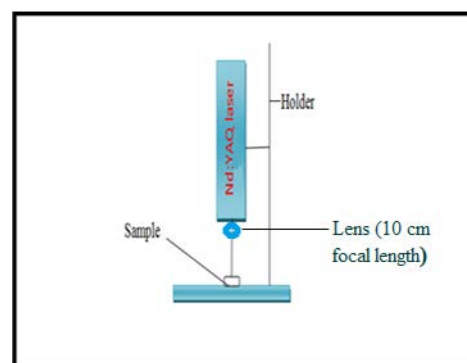

Figure 1: Experimental set-up.

*Corresponding author: Narges Zamil, Applied Sciences Department, University of Technology, Baghdad, Iraq, E-mail: ner_ner2@yahoo.com

Laser Induced Shock Wave Procedure

The working setup was based on a Nd: YAG laser operating at a wavelength of 1.06 μm and guided by red diode laser pointer. The emitted laser power can produce high laser intensity (10^{13} W/m²) formed a plasma and subsequently shock wave generation; as shown in Figure 2. This is usually associated with a rapidly expanding gas; associated with a strong pressure wave, a shock wave, emanating from the breakdown volume [1]. When reaching the free surface, the pressure wave creates surface waves on the substrate surface. The spatial and temporal profile of the surface waves contains information on the location and shape of the breakdown volume [2].

The material was irradiated by single and multi-pulses (2 to 5) for different laser energy (50 to 400) mJ on different materials.

XRD need long length and large irradiated area, to cover large areas, the laser irradiates pulses were made to In many rows with 50% overlapping ratio the set-up of overlapping ,overlapping system is shown in Figure 3.

The laser intensity (power density) was measured by using equations (2.20). The spot area was measured by using carbon material because it absorption is high and has small diffusivity rather than other materials. The laser spot on carbon is shown in Figure 4.

The used Nd: Yag laser given energy in voltage the calibration and converted from voltage to joule achieved by using Joulemeter Genetic type. Table 1 show the laser energy and intensity values.
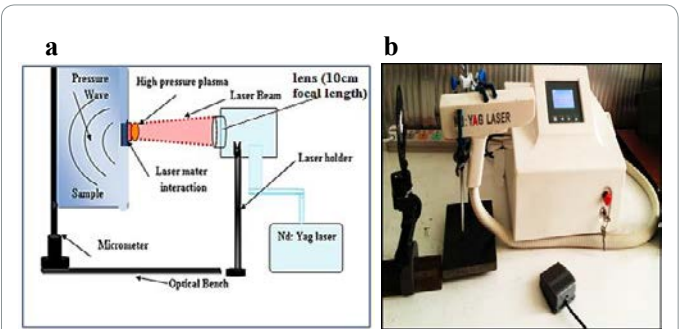

Figure 2: The experimental procedure set up, (a) sketch and (b) photographic image.
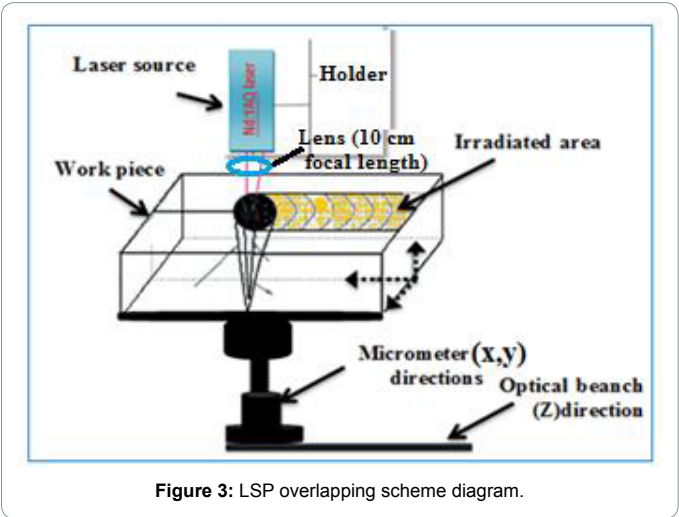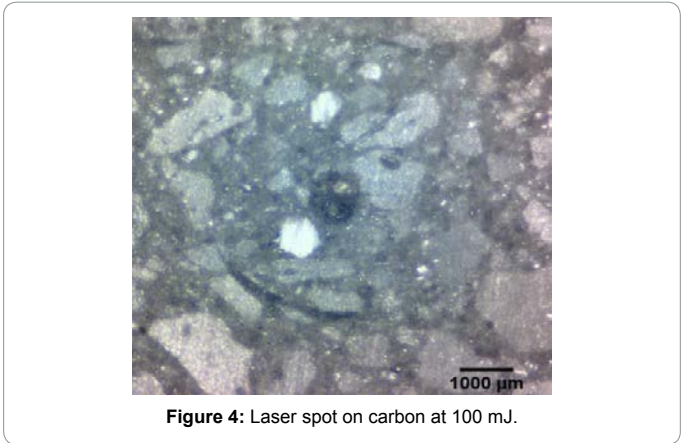

Figure 3: LSP overlapping scheme diagram.

Figure 4: Laser spot on carbon at 100 mJ.

Laser operation voltages	Laser energy (mJ)	I=×10^{13} W/m²
550	50	1.5
600	100	3.1
650	150	4.6
700	200	6.1
750	250	7.6
800	300	9.2
850	350	10.7
900	400	12.2

Table 1: Laser intensity calculations using 10 cm focal length lens. The averaged spot diameter was 0.8 mm and its cross-sectional area is 0.005 cm².
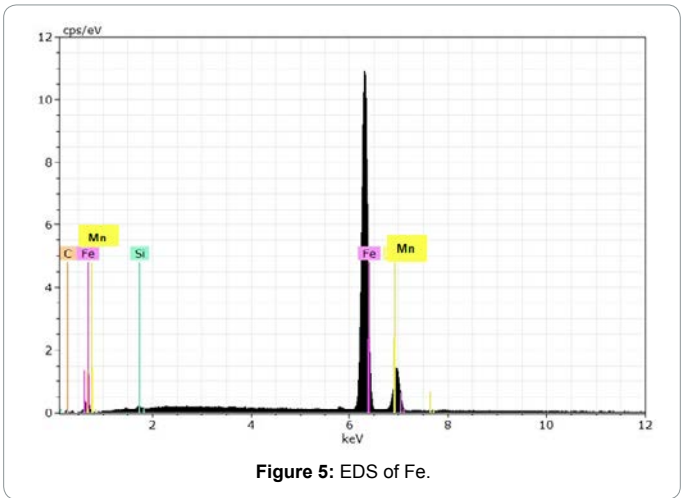

Figure 5: EDS of Fe.

X-ray diffraction analyses (XRD) were achieved in Nanotechnology and Advance Material Research Center in Al-Technology University.

Results

The effect of LSP on different material in a different media like air and water. This study includes (structure properties by using x-ray diffraction, shock wave parameters like (shock wave pressure, particle velocity, and shockwave velocity) where calculated.

Energy dispersive spectroscopy and X-ray diffraction analysis of Iron before and after LSP

The energy dispersive spectroscopy (EDS) of Fe is shown in Figure 5. The concentration of elements in the used sample is shown in Table 2. Figure 6 shows the XRD of Fe before and after LSP in different media by using different laser intensities for the unshocked sample

EI	Fe	Mn	C	Si
Norm. wt.%	79.51	17.17	2. 76	0.57

Table 2: The used Iron samples elements concentration.

Figure 6: Laser induced shock wave of Fe (a) without treatment, shocked in air at (b) 100 and (c) 200 mJ.

Figure 7: laser induced shock wave of Fe (a) without treatment, shocked in water at (b) 100 and (c) 200 mJ.

	2 Theta θ1	2 Theta θ2	2 Theta θ3	d(A) θ1	d(A) θ2	d(A) θ3	FWHM θ1	FWHM θ2	FWHM θ3
Without shock	44.83	65	82.37	2.02	1.434	1.17	0.621	0.754	0.784
100 mJ air	45.13	65.64	-	2.01	1.424	-	0.806	1.017	-
200 mJ air	45.02	-	82.52	2.01	-	1.168	1.076	-	1.976
100 mJ water	45.21	-	83.02	2	-	1.162	1.079	-	1.017
200 mJ water	45.01	-	82.77	2.013	-	1.165	1.002	-	1.448

Table 3: Iron diffraction angle, inter planer spacing and fall width half maximum before and after LSP.

Figure 8: EDS of S.S.304.

the FeO group is a presenced with high intensity and decreased after laser treatment, it means the laser cleaned Fe layer from native oxygen. Also, that means the change in atomic mass is happened where the particles with high atomic mass give more intense XRD in this case the (FeO has higher atomic mass than Fe) [3]. The Fe shocked in air with different laser intensity, the new peaks appeared in 100 mJ laser energy component due to the formation of Fe_2O_3 and disappeared at 200 mJ laser energy due to high laser energy evaporate or removed this component [4], smaller shifting in diffraction angle due from increasing in lattice parameter. The Fe peaks were decreased with increased laser energy because the phase transition of Fe will happen from Martensite to Austenitic (Martensite has a particle size greater than Austenitic) [5].

Figures 7 represents the material shocked under water at 100 and 200 mJ respectively, the oxide has lower intensity than fresh sample, in Table 3 the diffraction angle little shift toward higher diffracted rather than fresh samples and constant with small broadening in 200 mJ due to (the strain and ductility effect) [6].

Energy dispersive spectroscopy and X-ray diffraction of Stainless steel 304 before and after laser-induced shock wave process

The energy dispersive spectroscopy (EDS) of S.S.304 is shown in Figure 8 and Table 4.

Figure 9 represents S.S.304 shocked in air by 100 and 200 mJ. At low temperatures (550-600) K the Ferrite (α-Fe) is presence in S.S.304, by increasing laser energy Austenite peaks appeared with high intensity due to phase transition because of the high generated temperature [7].
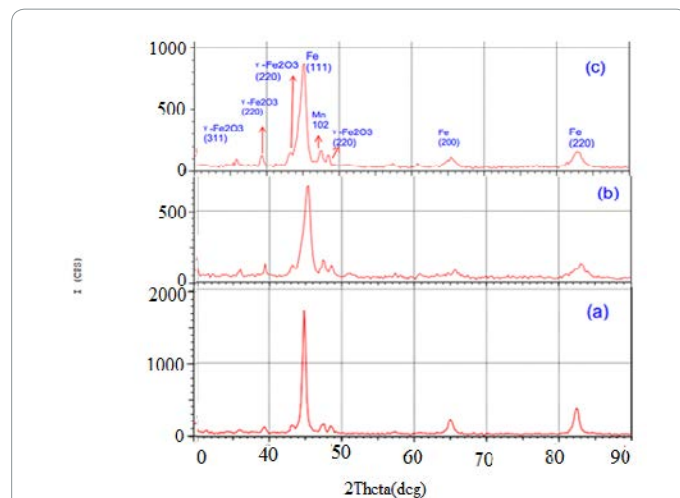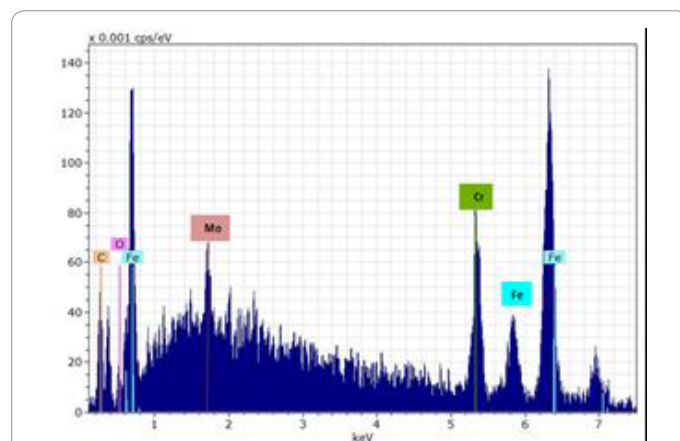
At 900°C typical low-carbon steel is composed entirely of Austenite, a high-temperature phase. At a temperature lower than 700°C, the austenite is thermodynamically unstable and, under equilibrium conditions, it will (undergo a eutectoid reaction and form pearlite) [8].

A shifting in diffraction angle happened toward small angle because of the substantial residual stress due to volume change on reaction. A compression happened to inner direction lead to decrease the lattice constant, also because of a phase transformation is taken place, a

twining is a dominant deformation mechanism by serve a plastic deformation of the grain refinement [9].

Figure 10 represents stainless steel is shocked by 100 mJ, and 200 mJ in water medium respectively, the diffraction angle little shift towards smaller angle rather than unshocked sample due to the smaller lattice constant, and phase transition the stress that generated due to higher generated shock pressure [10].

Under water the (γ -Fe$_2$O$_3$) has high intensity due to quenching and phase transition also high generated temperature changed magnetism from paramagnetic to ferromagnetic type that effect to XRD shifting and intensity as shown in Table 5.

Structure Parameters

From X-ray diffraction, we obtain the results given in Tables 4-7.

Grain size

Since the size of grains directly affect the on structure and hence

Figure 9: Laser-induced shockwave of S.S.304 (a) without treatment, shocked in air at (b) 100 and (c) 200 mJ.

properties of materials. Crystals are regular arrays of atoms, and X-rays can be considered waves of electromagnetic radiation. Atoms scatter X-ray waves, primarily through the atoms' electrons. A few specific directions, determined by Bragg's law:

$$2d \sin \theta = n\lambda \tag{1}$$

Here d is the spacing between diffracting planes, θ is the incident angle, n is any integer, and λ is the wavelength of the beam. The relation between the inter planer spacing and lattice constant (a) is given by [11]:

$$d = \frac{a}{\sqrt{h^2 + k^2 + l^2}} \tag{2}$$

The grain size was calculated from Sherrie eq. given by [12]:

$$D_{hkl} = \frac{K \lambda}{B \cos\theta} \tag{3}$$

Where B is the integral half width, K is a constant equal to 0.94, λ is the wavelength of the incident X-ray (λ=0.15406 nm), D is the crystallite size, and θ is the Bragg angle. Its value is shown in Table 6 for used materials as follow:
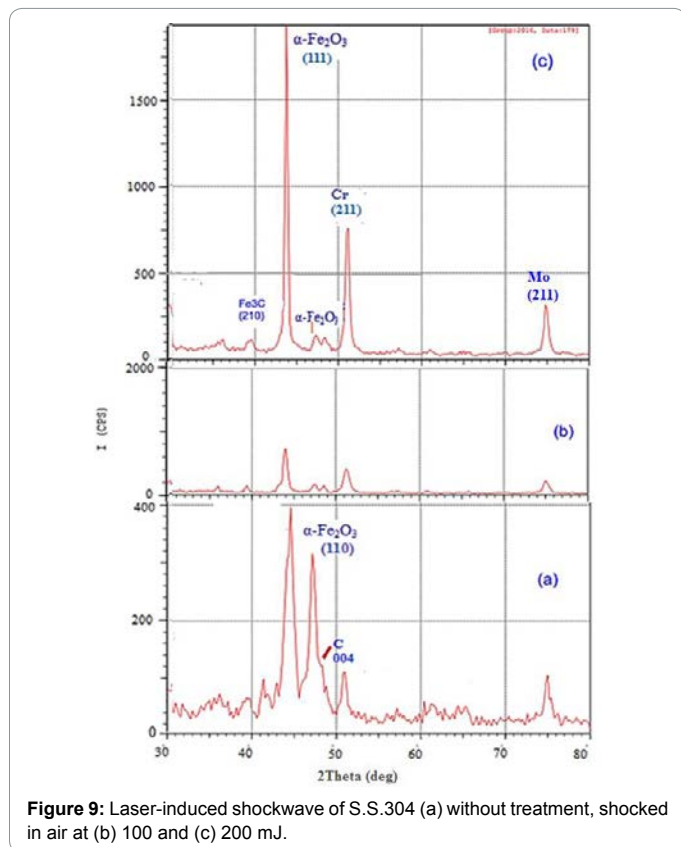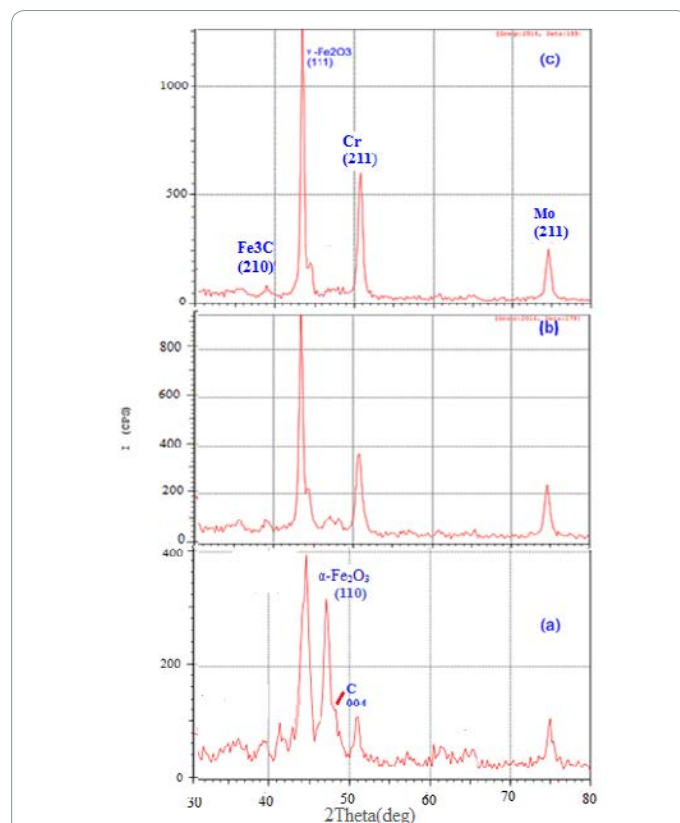

Figure 10: Laser-induced shockwave of S.S.304 (a) without treatment, shocked in water medium at (b) 100 mJ and (c) 200 mJ.

El	Fe	Cr	Mo	C	O
Norm. wt.%]	68.83	12.98	11.3	0	0.58

Table 4: The used S.S. 304 samples elements concentration.

	2 Theta θ1	2 Theta θ2	2 Theta θ3	d(A) θ1	d(A) θ2	d(A) θ3	FWHM θ1	FWHM θ2	FWHM θ3
Unshock	44.45	50.94	74.92	2.04	1.79	1.267	1.16	0.62	0.72
100 mJ air	44	51.26	75.01	2.06	1.78	1.265	0.65	0.78	0.77
200 mJ air	43.8	51.07	74.83	2.07	1.79	1.268	0.54	0.65	0.66
100 mJ water	43.44	50.72	74.57	2.08	1.8	1.27	0.61	0.84	0.79
200 mJ water	43.45	50.74	74.58	2.08	1.8	1.27	0.598	0.77	0.74

Table 5: S.S.304 diffraction angle, inter planer spacing and fall width half maximum before and after LSP.

Sample condition	Fe	S.S.304
Unshocked	13.86	12.33
100 mJ air	10.43	13.16
200 mJ air	6.97	15.48
100 mJ water	9.61	12.89
200 mJ water	8.3	13.47

Table 6: Grain size (nm) of used samples.

Sample condition	Fe	S.S.304
Unshocked	0.0052	0.0074
100 mJ air	0.0077	0.0061
200 mJ air	0.0106	0.0052
100 mJ water	0.0082	0.0063
200 mJ water	0.0089	0.0068

Table 7: Lattice strain of used samples.

Material	constant (a) (Km/s)	Constant (b)	Impedance (kgm^{-2}s^{-1} × 10^6)
Fe	3.574	1.920	46.4
Stainless steel 304	4.580	1.49	45.7

Table 8: Acoustic impedance, and (a) and (b) constants value of different metals.

Grain size of Fe: The grain size of Fe in air is decreased after LSP due to phase transition from Martensite to Austenite that has smaller grain size. In water the decreased of grain size due to quenching led to phase transition to Martensite differs from old one by has smaller grain size.

Grain size of S.S.304: The grain size in air increased due to both multidirectional mechanical twins and multidirectional Martensite bands led to grain refinement mechanism this consisted with [13]. In water the shock pressure is greater than in air, the distortion becomes stronger and stronger, finally the accumulated distortion make the original twin into intercrossed.

Lattice strain

The strain-induced broadening due to crystal imperfection and distortion was calculated using the formula:

$$\varepsilon = \frac{B_{hkl}}{4tan\theta} \tag{4}$$

Fe lattice strain: in air lattice strain increased with increasing laser energy due to cold working that induced by plastic deformation of materials. The shocked Iron in water medium, is exposed to the quickly quenching led to increasing the ductility between the particles rather than a fresh sample, but shocked material under water is smaller than shocked it in the air due to increased shock pressure when samples shocked in water [1,5].

S.S.304 lattice strain: in air, lattice strain decreased with increased laser energy due to Martensite transitions, In water the decreasing of lattice strain due to increased heating led to increased diffusion enhanced dislocation motion, decreased dislocation density by annihilation, formation of low energy dislocation configurations, relieve of the internal strain energy (Table 7).

Dislocation densities

The dislocation density (δ), the dislocation toughly influences many of the properties of materials, which represents a number of defects in the sample is defined as the length of dislocation lines per unit volume of the crystal and is calculated using the equation,

$$\delta = \frac{1}{D_{hkl}^2} \tag{5}$$

Where D_{hkl} is the crystallite size.

Fe dislocation density: After shocked Fe the dislocation is increased with increasing laser intensity in different media (air and water), due to temperature effect also because of cold working that induced by deformation of materials.

S.S.304 dislocation density: In air and water decreasing dislocation density with increasing laser energy due to twining effects.

Laser Shock Wave Properties

This includes shock wave pressure particle velocity, and shock wave velocity.

Shockwave pressure

The pressure value; due shock wave effect could be measured when the size of the Gaussian laser beam is relatively great. The shock model makes modifications to Fabbro's model after assuming that the laser beam spot size in the order of microns. The 1-D assumption is followed, but 2-D equivalence is considered to account for the small laser spot size [1].

$$P = (AZI)^{1/2} \tag{6}$$

$$Z = \rho * V_l \tag{7}$$

Where, Z: acoustic impedance of material, ρ: density V_l: velocity of acoustic waves in the material. When using a confining medium, the acoustic impedance $z = \dfrac{2}{\left(\dfrac{1}{z1} + \dfrac{1}{z2}\right)}$ is expressed in terms of those of the confining medium (z_1) and the target material (z_2).

and illustrated in Table 8. The shock pressure is increased with increasing the laser intensity due to increase surface temperature so increased the number of ions that emerged from the irradiated surface [1], Shock pressure of ferrite metals (Fe) is greater than S.S.304). That means increased pressure with increased magnetism of metals due to increased acoustic impedance. A shock pressure for all metals is great in water than in air medium due to the shock wave that generated by laser is wave that is transferred by particles science particles are spread so far a part in gas. Water is incompressible; particles are together and give impedance to applied force greater than air consequently increased shock pressure. The shock pressure depending on absorption [1] (Figure 11).

Shock velocity and particle velocity

When a laser pulse of high energy interacts with the material, the hot plasma is produced which is expanding at very high speed in the opposite direction of the laser. Externally expanded plasma utilizes high pressure in the direction of the interior, to form a wave of severe shock towards the interior. P is shocked pressure, V_L is shocked velocity, and V_p is the partial velocity. The relation between particle velocity and shock pressure related with acoustic impedance (Z), and given as flow:

$$V_p = \frac{P}{Z} \tag{8}$$

The Shockwave velocity and particle velocity related to each other tor as:
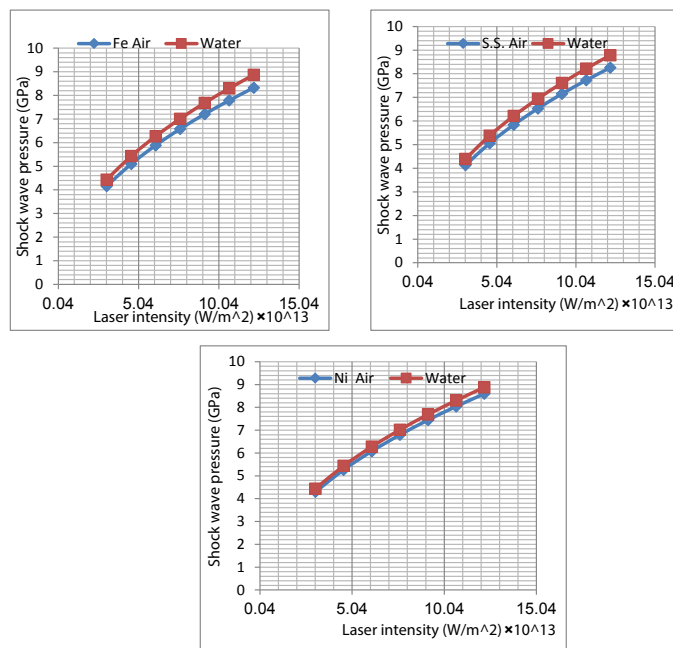
$$V_l = a + bV_p \tag{9}$$

Figure 11: Laser-induced shockwave pressure vs. laser intensity at different metals at air, water, and ethanol media.
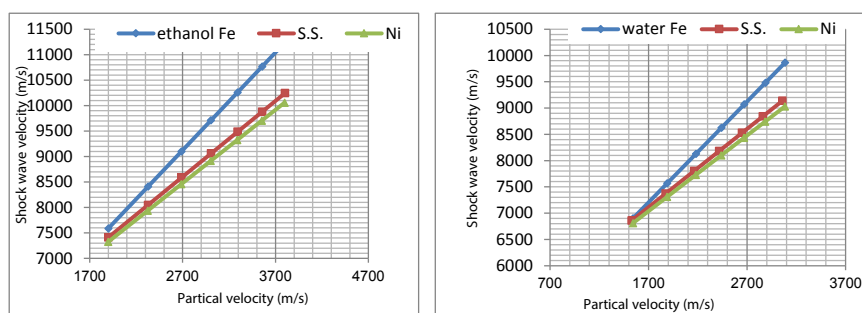

Figure 12: Laser-induced shockwave velocity vs. particle velocity.

Where *a* and *b* is constant given in Stanley *P*. Marsh data book and shown in the Table 8. Figure 12 shows particle velocity.

A linear relation between shock velocity and particle velocity for all metals in different media is observed because of the dependence on each other. Shock velocity is great in water and ethanol than in air, because (the acoustic impedance of air is smaller than water and ethanol), the shock and particle velocity is affected by temperature when laser intensity is increased the temperature increased so shock wave tend to travel faster at height temperatures.

Conclusions

Laser induced shock wave field is a very interesting area of study. It turns out to be a very useful non-destructive technique to study the material properties especially with very small area. We can summarize the main conclusions of our work as follow; LSP is a successful method to increase the hardness of some metals. LSP is a simple, low cost and controllable. X-ray diffraction showed a reduction in the grain size after the shocking process. The deformation increased after LSP process and this means increased ductility of metals. This effect led to increased dislocation density and enhanced stress.

References

1. Gujba AK, Medraj M (2014) Laser peening process and its impact on materials properties in comparison with shot peening and ultrasonic impact peening. Materials 7: 7925-7974.

2. Gornikowska MR, Kusinski J, Blicharski M (2011) The Influence of The Laser Treatment on Microstructure of the Surface Layer of an X5CrNi18-10 Austenitic Stainless Steel. Archives of Metal Allergy and Materials 56: 717-721.

3. Clauer A (1997) Laser Shock Peening For Fatigue Resistance. J Metal Society 18: 217-230.

4. Jay FT, Alexander GP (2007) Low Speed Laser Welding of Aluminum Alloys Using Single-Mode Fiber Lasers. J. Welding 86: 179-186.

5. Callisster WD (2006) Materials Science And Engineering. An Introduction. John Wiley and Sons, Inc., 200-252.

6. Bo H, Ma Z, Jing X, Ting YY (2011) Structural Electrical and Optical Properties of Azo/Sio2/P-Si SIS Heterojunction Prepared by Magnetron sputtering. J Optical Applicant 11: 15-24.

7. Ameen HA, Hassan KS, Mubarak EM (2011) Effect Of Loads, Sliding Speeds and Times on the Wear Rate for Different Materials. American J Science and Industrial Research 2: 99-106.

8. Young DA (1975) Phase Diagrams of the Element. Lam/Lam/Hencehunermofe Laboratory 20: 21.

9. Bindu P, Thomas S (2014) Estimation of Lattice Strain in Zno Nanoparticles: X-Ray Peak Profile Analysis. J Theor Appl Phys 8: 123-134.

10. Cheng YT, Cheng CM (1998) Scaling Approach to Conical Indentation in Elastic-Plastic Solids with Work Hardening. J Appl Phys 84: 1284-1291.

11. Vogel A, Busch S (1996) Shock Wave Emission And Cavitation Bubble Generation by picosecond and nanosecond optical breakdown in water. J. Acoust. Soc. Am 100: 148-165.

12. Ariga S, Sigel R (1976) Picosecond Microphotography as a Diagnostic Method for Laser Produced Plasmas. 31: 697-706.

13. Marsh P (1980) Lasl Shock Hugoniot Data. The Regents of the University of California, USA 89: 110-212.